Physics of the Earth and Planetary Interiors 240 (2015) 95–104

Contents lists available at ScienceDirect

Physics of the Earth and Planetary Interiors

journal homepage: www.elsevier.com/locate/pepi

Deformation of forsterite polycrystals at mantle pressure: Comparison with Fe-bearing olivine and the effect of iron on its plasticity

Caroline Bollinger [1], Sébastien Merkel *, Patrick Cordier, Paul Raterron

Unité Matériaux Et Transformations (UMET), CNRS, Université Lille 1, F-59655 Villeneuve d'Ascq, France

ARTICLE INFO

Article history:
Received 7 April 2014
Received in revised form 4 September 2014
Accepted 2 December 2014
Available online 23 December 2014

Keywords:
Olivine
Forsterite
Rheology
Aggregate
Dislocation creep
High pressure
D-DIA
Stress exponent
Activation volume

ABSTRACT

The rheology of polycrystalline forsterite was investigated in the Deformation-DIA (D-DIA) using *in situ* X-ray diffraction at pressure between 3.1 and 8.1 GPa, temperature in the 1373–1673 K range, and at steady-state strain rate ranging from 0.5×10^{-5} to 5.5×10^{-5} s^{-1}. Microscopic observations of the run products show characteristic microstructures of the so-called "dislocation creep regime" in wet conditions. Based on the present data at 1473 K, the pressure effect on forsterite plasticity is quantified using an activation volume $V^*_{Fo} = 12.1 \pm 3.0$ cm^3 mol^{-1}. A comparison between the strain rates of San Carlos olivine and forsterite specimens deformed together indicates that, at the experimental conditions, they compare with each other within less than half an order of magnitude. This comparison also allows for the determination of the stress exponent of forsterite of $n_{Fo} = 2.3 \pm 0.6$. Our results, combined with data from the literature, indicate a clear trend of increasing stress exponent with Fe content in olivine.

© 2014 Elsevier B.V. All rights reserved.

1. Introduction

Olivine $(Mg,Fe)_2SiO_4$ is the main constituent of the Earth's upper mantle and, more generally, of the mantle of terrestrial planets. As such, the rheology of olivine-bearing rocks is relevant for constraining the dynamics occurring within these bodies. Olivine rheology depends on multiple parameters. The effect of temperature (T) and differential stress (σ) have long been quantified (*e.g.*, Bai and Kohlstedt, 1992; Hirth and Kohlstedt, 2003). More recently, it has also been shown that pressure (P), within the range in Earth's upper mantle, has a significant influence on olivine deformation mechanisms (*e.g.*, Bollinger et al., 2014 and references therein).

Composition, also, is an important parameter. At the scale of a rock, other components such as pyroxenes (*e.g.*, Bystricky et al., 2006; Raterron et al., 2014) or small melt fractions (*e.g.*, Hirth and Kohlstedt, 1996; Mei et al., 2002; Holtzman et al., 2003) can affect significantly the mechanical properties. At the microscopic scale, the plastic response of olivine is sensitive to the oxygen fugacity (fO_2), crystal hydroxyl content [OH] (*e.g.*, Girard et al., 2013), and iron content (Hitchings et al., 1989; Katayama and Karato, 2008; Zhao et al., 2009; Nishihara et al., 2014). In the Earth's mantle, olivine Fe number (Fe#) – the Fe/(Mg + Fe) atomic ratio – ranges between 4% and 13% (Deer et al., 1992, p. 12). The Martian mantle is expected to be significantly richer in iron with Fe# estimated between 20% and 25% (*e.g.*, Khan and Connolly, 2008; Ruedas et al., 2013). Among the few studies devoted to the influence of iron on the olivine rheological properties, fewer have addressed the influence of this parameter at $P > 3$ GPa (Nishihara et al., 2014).

Here we report results from deformation experiments performed at P and T up to 8.1 GPa and 1673 K, respectively, on iron-free olivine polycrystals, *i.e.*, pure forsterite (Fo100) aggregates. We then quantify the rheology of forsterite at mantle conditions. Finally, we analyze the effect of iron content on olivine plasticity by comparing forsterite and San Carlos olivine specimens deformed at identical conditions.

2. Experimental details and run product microstructures

Deformation experiments were performed in the Deformation-DIA apparatus (D-DIA, Durham et al., 2002; Wang et al., 2003) at the X17B2 beamline of the National Synchrotron Light Source (Upton, NY, USA), at P ranging from 3.1 to 8.1 GPa, T in the range 1373–1673 K and at controlled strain rates $\dot{\varepsilon}$ ranging from 0.5×10^{-5} to 5.5×10^{-5} s^{-1} (Table 1). Bollinger et al. (2014)

* Corresponding author.
E-mail address: sebastien.merkel@univ-lille1.fr (S. Merkel).
[1] Present address: Bayerisches Geoinstitut, University of Bayreuth, 95440 Bayreuth, Germany.

http://dx.doi.org/10.1016/j.pepi.2014.12.002
0031-9201/© 2014 Elsevier B.V. All rights reserved.

reported details on the experimental set up, data analysis, and results for olivine. The following section is hence limited to the most relevant information regarding the present results.

2.1. Starting material, run a_{Opx} and fO_2 conditions

The forsterite starting material was prepared by crushing one gem quality single crystal of Fo100 in an alumina-mortar, grinding it to a fine-grained powder at the optical scale (average grain size ~10 μm). The starting crystal was synthesized at room pressure by the Czochralski (CZ) process (*e.g.*, Takei and Kobayashi, 1974). It was dry, *i.e.*, no hydroxyls were detectable using Fourier's transform infrared spectroscopy (FTIR, see Raterron et al., 2007).

Specimens were loaded into the D-DIA deformation cell (Fig. 1) in between two machinable alumina end plugs, which become hard pistons at run conditions. Two types of experiments were performed. Runs #65, #68, #69, #70 were carried out with one sample of pure forsterite powder in the compression column. Runs #80, #81, #82, #87, #88, #89 and #90 were performed with two powder samples, one of pure forsterite and one of San Carlos olivine atop one another, separated by a thin layer of alumina sandwiched in between Re foils. Both forsterite and olivine powders were mixed with a small fraction (5 wt.%) of natural enstatite (En84Fs13Wo3) powder, in order to buffer the orthopyroxenes (Opx) activity ($a_{Opx} = 1$) and limit grain growth during the runs (McDonnell et al., 2000). Although Fe–Mg exchanges must have occurred during the runs, mostly at contacts between enstatite and forsterite grains, they were limited by the Fe–Mg interdiffusivity in enstatite which is lower than that in olivine (diffusion rates of ~0.1 μm/h at $T = 1673$ K, Ganguly and Tazzoli, 1994; Jaoul et al., 1995). Given the run temperatures, durations, the enstatite grain size (several microns) and small fraction, the amount of iron which can diffuse into forsterite grains during the runs is negligible, *i.e.*, it cannot significantly affect the forsterite composition (Fo100).

The oxygen fugacity (fO_2) was not controlled during the runs. This is because encapsulating the specimens into metal/metal-oxide jackets reduces the accuracy of differential-stress (σ) measurements by X-ray diffraction. Indeed, such capsules typically have a strong absorption coefficient in the 10–40 keV energy range of the X17B2 beamline. Moreover, the strong diffraction peaks from the metal jacket could hide essential information from material of interest. This is not an issue for forsterite for which rheology is essentially fO_2 insensitive. Unlike forsterite, San Carlos olivine plasticity is sensitive to fO_2 (*e.g.*, Keefner et al., 2011). However, as reported in Bollinger et al. (2014), olivine run products do not exhibit silica-rich or metallic micro-precipitates related to oxidation or reduction, attesting that these samples remained within the olivine Redox stability field during deformation.

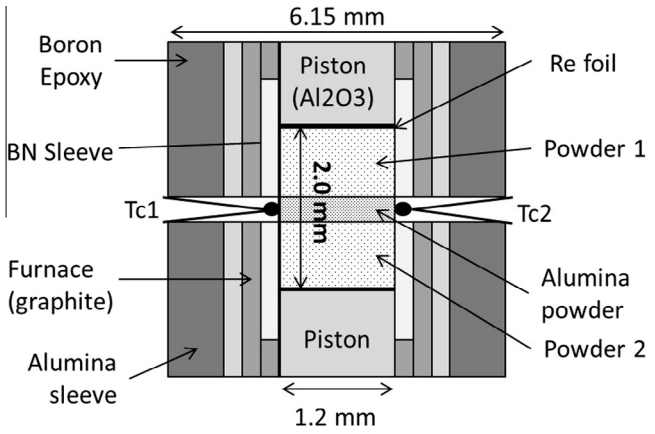

Fig. 1. Cross-section of the cell assembly used for the experiments. Olivine and forsterite samples, separated by an alumina buffer, are studied simultaneously. Tc1 and Tc2 are thermocouples in contact with the alumina. Re foils are used to monitor samples strain using X-ray radiography. This paper focuses on forsterite rheology. Results regarding olivine rheology have been published in Bollinger et al. (2014).

2.2. In situ strain, pressure, differential stress and temperature measurements

Specimen strain (ε) and strain rate ($\dot{\varepsilon}$) were measured from the positions of metal foils placed at sample ends (Fig. 1) by time-resolved X-ray radiography (Vaughan et al., 2000). The distance between the foils was measured by eye at given horizontal positions on the radiographs and used as a proxy for specimen lengths. Beside the image pixel resolution, sources of uncertainties using this method are the possible rotation and/or thinning of the foils during deformation. However, significant rotations of the foils relative to the several percent specimen strains would have been detected visually. Using hard Re foils also prevents significant thinning of the strain markers during deformation. The obtained strain rates and corresponding uncertainties are reported in Table 1.

Taking advantage of the ten-element energy-dispersive multi-detector (Weidner et al., 2010), P and σ were measured *in situ* from d-spacing variations for given reflections in different orientations with respect to the principal stress directions. Following the protocol reported in Bollinger et al. (2012), alumina 012, 104, 110, 113, 024 and 116 first-order diffraction lines were used along with thermal expansion coefficients from Fei (1995), elastic moduli and thermal derivatives of Anderson and Isaak (1995), and the pressure derivatives of Duan et al. (1999). The calculation is based on a purely elastic model (Singh et al., 1998), which does not account for stress heterogeneities or relaxation induced by plastic deformation (Merkel et al., 2009). Consequently, different σ values are obtained from different *hkl* lines. More sophisticated approaches based on elasto-plastic self-consistent (EPSC) modeling can be used to measure more accurately the "true-σ" and, in the case of alumina, Raterron et al. (2013) showed that averaging *hkl*-line stresses leads to reasonable estimates. Stresses reported in Table1 for the sample, top, and bottom pistons are hence calculated using a weighted mean of all *hkl*-line stresses for each. Errors on individual *hkl*-stresses are propagated to obtain a first source of error on the specimen mean stress (resulting from the accuracy of the measurement). We then calculate the standard deviation of all measured *hkl*-stresses for each specimen (error resulting from the physical model). In a conservative approach, we finally assume that the total error on σ for each specimen is the sum of these two values.

Temperature was measured using two horizontal W3%Re–W25%Re thermocouples (no pressure correction) whose junctions were placed at the centre of the cell assembly (Fig. 1). Run T uncertainty is mostly due to axial thermal gradients, which can be in excess of ~150 K/mm at high T at the centre of the cell (Raterron et al., 2013). Given the present run nominal T, and the size and vertical position of our specimens, we estimate T uncertainty to ±100 K.

Pressure was measured in the pistons using the parameters listed above. It was also measured in the forsterite specimens using 021, 101, 002, 130, 131, 112 and 041 diffraction lines and equation of state (EoS) parameters extracted from Isaak et al. (1989) and Zha et al. (1996). For each material, pressures reported in Table 1 are weighted mean values of all pressures measured during steady-state. When measuring the cell pressure in the pistons from an EoS, thermal axial gradients cannot be omitted (Raterron et al., 2013). Here, we assume that the specimen nominal T was that measured (or previously calibrated) with the thermocouples, and that the pistons T was 200 K lower. In some cases, we observe large

Download English Version:

https://daneshyari.com/en/article/4741541

Download Persian Version:

https://daneshyari.com/article/4741541

Daneshyari.com